18th International Congress on Artificial Materials for Novel Wave Phenomena – Metamaterials 2024
Crete, Greece, Sep. 9th –14th, 2024

Experimental Realization of the Slepian-Pollak Tomographic Imaging: Super-Resolution for Limited-size Objects

T. Chang [1], G. Adamo [1], J. So [1], E. A. Chan [1], N. Papasimakis [2], Y. Shen [1], N. Zheludev [1,2]

[1] Centre for Disruptive Photonic Technologies, SPMS and TPI, Nanyang Technological University, Singapore 637371, Singapore
[2] Optoelectronics Research Centre and Centre for Photonic Metamaterials, University of Southampton, Southampton, SO17 1BJ, UK
taeyong.chang@ntu.edu.sg

Abstract **– We report a new imaging concept that — in principle — allows unlimited optical resolution of a limited-size object. The image reconstruction is a reversed process to superoscillatory focusing where a mask can be designed to focus light into subwavelength hotspots of any size and shape. The imaging is based on *individually* measuring coefficients of the Slepian-Pollak decomposition of the light field scattered by the object. Here high resolution is possible because the weak components of decomposition that are responsible for the object's fine details can be measured with high signal-to-noise ratios by integration. Then the limited-size object is reconstructed by back-propagating as the Slepian-Pollak functions are orthogonal within the limited size range of interest with spatial frequencies limited by the free space wave-vector. We report a proof-of-principle experimental demonstration of this concept with two-dimensional nano-objects achieving resolution exceeding λ/6.**

I. INTRODUCTION

Achieving super-resolution in label-free far-field (L3F) optical imaging is still a challenging problem. Despite the importance and high demand for super-resolution imaging, the majority of the available techniques rely on nonlinearity and/or labelling of specimens. Here we introduce a tomographic imaging that reconstructs an image using a Slepian-Pollak series decomposition of the scattered light, an orthonormal basis different from the Fourier series which is conceptually described in Fig. 1a. We introduce a statistical point spread function as a resolution criterion where the estimation of each component of the series is allowed, and the effect of the element-wise signal-to-noise ratios (SNR) on the image resolution is characterized (Fig. 1b). We show that the proposed imaging technique can, in principle, achieve arbitrarily fine resolution, and it has the same generality of conventional Fourier imaging, with the only restriction being a finite region of interest (ROI). In the experiment, we performed sequential tomography using a digital micromirror device. We built a shot-noise-limited setup and measured appropriately longer to achieve the desired SNR. We experimentally demonstrate imaging of nanoparticles with a resolution comparable to conventional Fourier imaging with numerical aperture NA = 3.

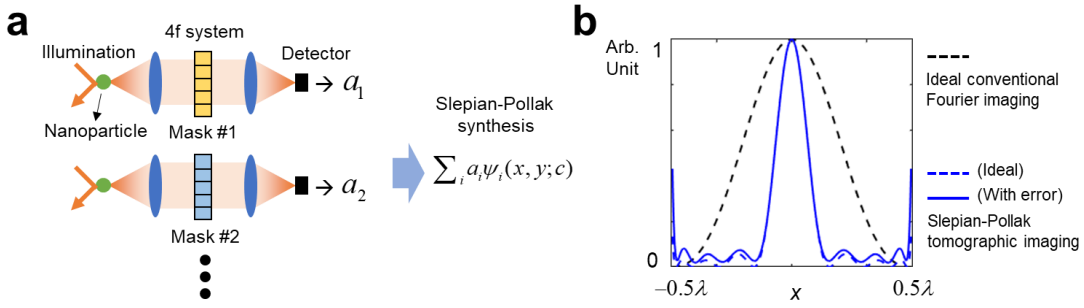

Fig. 1. (a) Concept of the Slepian-Pollak tomographic imaging where $\psi_i(x,y;c)$ is the i-th Slepian-Pollak function. (b) Statistical point spread functions for Fourier imaging and Slepian-Pollak tomographic imaging.

II. Result and Discussion

A. Imaging with Slepian-Pollak series as a reciprocal process of superoscillatory hotspot generation

Any arbitrary function defined within an interval can be approximated, with arbitrarily good precision, using the Slepian-Pollak series, built using prolate spheroidal wave functions. The Slepian-Pollak functions, $\psi_i(\mathbf{x};c)$ and $\psi_i(\mathbf{k};c)$, are eigenfunctions of finite Fourier transform:

$$U(\mathbf{x}) \approx \sum_{i=0}^{N} a_i \psi_i(\mathbf{x};c) \quad \xrightarrow{\text{finite } \mathcal{F}} \quad \sum_{i=0}^{N} a_i \gamma_i(c) \psi_i(\mathbf{k};c) \tag{1}$$

where c, and $\gamma_i(c)$ are the ROI-bandwidth parameter and the eigenvalues for the finite Fourier transform, respectively. In the case of an optical field, $a_i\gamma_i(c)$ can be measured in the far-field since they are coefficients of bandlimited functions, and a_i can be directly estimated with known $\gamma_i(c)$, which enables the synthesis of $U(\mathbf{x})$.

This Slepian-Pollak imaging can be understood as a reciprocal process of well-known superoscillatory hotspot generation [1]: to generate a hotspot of arbitrary shape within the ROI, the target profile is approximated with finite Slepian-Pollak series followed by Fourier transform, which is then utilized to design the mask. By considering equivalent source profiles for both hotspot generation (Fig. 2a) and imaging (Fig. 2b), the two cases satisfy the Lorentz reciprocity theorem, i.e., $\langle E_1, J_2\rangle = \langle E_2, J_1\rangle$.

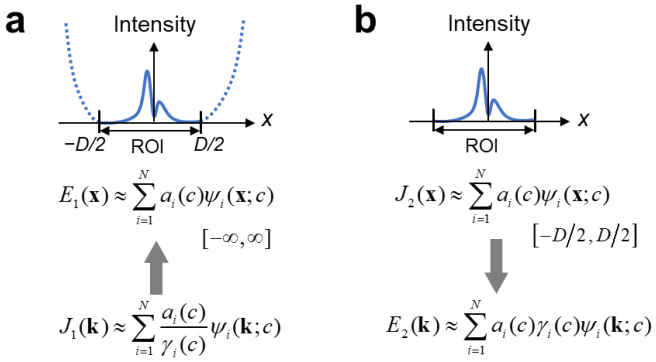

Fig. 2. (a) Superoscillatory hotspot generation. (b) Slepian-Pollak series of source and far-field radiation.

B. Statistical point spread function and signal-to-noise ratio requirement

The challenge of the proposed strategy lies in the fact that the higher the order of the Slepian-Pollak component, the weaker the energy transfer (i.e., smaller $\gamma_i(c)$ for larger i), which makes the measurement difficult to be accurate. To systematically overcome the challenge, we first quantify the resolution taking into account the effect of noise for each measurement of coefficient. The ensemble average of noisy point spread function, namely statistical point spread function (SPSF) for impulse source position $\mathbf{x}'$, can be written as

$$\mathrm{SPSF}(\mathbf{x};\mathbf{x}') = \lim_{R\to\infty} \frac{1}{R} \sum_{r=1}^{R} \langle \mathbf{x} | M^{(r)} | \mathbf{x}' \rangle \langle \mathbf{x}' | M^{(r)\dagger} | \mathbf{x} \rangle \tag{2}$$

where $M^{(r)}$ is r-th realization of the measurement operator. The matrix representation of $M^{(r)}$ with position basis becomes $G^{\dagger}T^{-1}(I+X^{(r)})TG$ where G, T, $X^{(r)}$, and I are generalized Fourier transform matrix, optical transfer matrix, diagonal noise matrix, and identity matrix, respectively. Figure 1b compares examples of SPSF(x;0) of conventional Fourier imaging with a numerical aperture (NA) of 1 without error (dashed black), Slepian-Pollak imaging with N=10 with (solid blue) and without error (dashed blue). $X^{(r)}$ with SNR of 10 for the first seven and 2 for the remaining components is utilized and D is assumed as the identity matrix for this example. Because the Slepian-Pollak basis forms a quasi-uniform grid [2], the shape of SPSF(x;x') is not much different from SPSF(x;0). Therefore, we claim that the full-width half-maximum of SPSF(x;0) can be considered as a resolution. It can be shown that the resolution of Slepian-Pollak imaging can be much finer than that of conventional Fourier imaging, and the SPSF profile is not much deteriorated with a reasonable degree of SNR.

C. Experiments

To achieve the target SNR, we establish a shot-noise-limited measurement process and increase the measurement times which are determined by the eigenvalues, $\gamma_i(c)$, and the distortion matrix that characterizes the optical distortion introduced by the optical setup. A schematic of the optical setup and the measured distortion matrix are shown in Fig. 3a and b, respectively. We utilize total internal reflection illumination on nanoparticles and perform sequential tomography of Slepian-Pollak modes. A sapphire cube is used as a prism for the TIR configuration and as a substrate for the sample at the same time. Platinum nanoparticles are fabricated on the sapphire cube by electron beam-induced deposition. The prolate spheroidal wave functions are realized with a digital micromirror device (DMD) placed at the back focal plane of an objective lens with NA=0.9 and their coefficients are measured sequentially (i.e., spatial-mode tomography [3]). Four images, with different illumination directions, are acquired and incoherently added to form the final image.

We establish a shot-noise-limited measurement process by implementing three steps. First, the DMD mask is used both as reference and signal to configure the common-path interferometry. The reference is much stronger than the detector noise, a necessary condition for shot-noise-limited measurements. Second, the focus plane is consistently maintained, through all the measurements for various samples, by operating the position metrology of the substrate using a second laser. Third, the microscope drift is compensated using the piezo stage, by running a real-time three-dimensional position estimation of the nanoparticles.

Figure 3c gives an overview of the performance of the technique, by comparing the experimentally measured images with the calculated ideal Slepian-Pollak imaging, ideal Fourier imaging with NA=1, and ideal Fourier imaging NA=3. The measured images, using 19 coefficients and an ROI diameter of 0.8λ, are comparable with those obtained from an ideal Fourier imaging with NA=3, setting a new state-of-the-art performance for optical label-free far-field imaging.

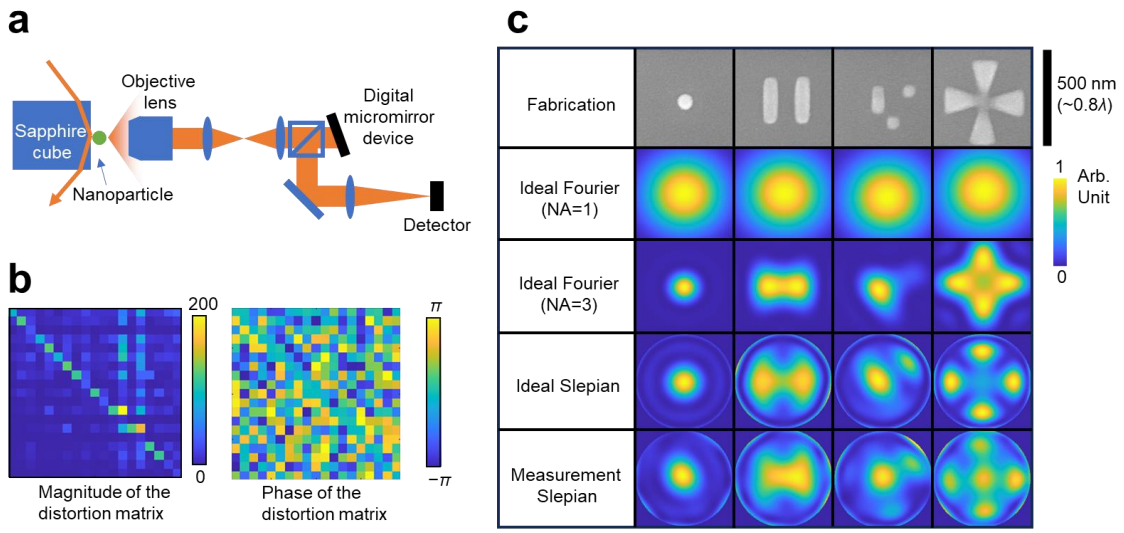

Fig. 3. (a) Schematic of the setup. (b) Measured distortion matrix. (c) Performance of Slepian-Pollak tomographic imaging.

III. Conclusion

We propose and realize a Slepian-Pollak tomographic imaging, a label-free far-field optical imaging technique that can achieve arbitrarily fine imaging resolution within a finite region of interest, and experimentally demonstrate $\lambda/6$ resolution.

References

[1] F.M. Huang and N.I. Zheludev, "Super-Resolution without Evanescent Waves," *Nano Lett.*, vol. 9(3), p. 1249-1254.
[2] J.P. Boyd, "Prolate spheroidal wavefunctions as an alternative to Chebyshev and Legendre polynomials for spectral element and pseudospectral algorithms," *J. Comput. Phys.*, vol. 199(2), p. 688-716, 2004.
[3] J. Pinnell *et al.*, "Modal analysis of structured light with spatial light modulators: a practical tutorial," JOSA A, vol. 37(11), p. C146-C160, 2020.